

## Lattice location and thermal stability of implanted Fe in ZnO

E. Rita,<sup>a),b)</sup> U. Wahl, J. G. Correia,<sup>b)</sup> and E. Alves

*Instituto Tecnológico e Nuclear, Estrada Nacional 10, 2686-953 Sacavém, Portugal and Centro de Física Nuclear da Universidade de Lisboa, Avenida Professor Gama Pinto 2, 1649-003 Lisboa, Portugal*

J. C. Soares

*Centro de Física Nuclear da Universidade de Lisboa, Avenida Professor Gama Pinto 2, 1649-003 Lisboa, Portugal*

The ISOLDE Collaboration

*CERN-PH, 1211 Geneva 23, Switzerland*

(Received 16 August 2004; accepted 23 September 2004)

The emission channeling technique was applied to evaluate the lattice location of implanted  $^{59}\text{Fe}$  in single-crystalline ZnO. The angular distribution of  $\beta^-$  particles emitted by  $^{59}\text{Fe}$  was monitored with a position-sensitive electron detector, following 60 keV low dose ( $2.0 \times 10^{13} \text{ cm}^{-2}$ ) room-temperature implantation of the precursor isotope  $^{59}\text{Mn}$ . The emission patterns around the [0001], [1102], [1101], and [2113] directions revealed that following annealing at 800 °C, 95(8)% of the Fe atoms occupy ideal substitutional Zn sites with rms displacements of 0.06-0.09 Å. © 2004 American Institute of Physics. [DOI: 10.1063/1.1825611]

Numerous technological breakthroughs are envisaged with the use of magnetic semiconductor materials that show a ferromagnetic ordering temperature at or above room temperature; for example, spin transistors, ultradense nonvolatile memories, and optical emitters with polarized output.<sup>1</sup> One class of materials that is especially promising for applications are diluted magnetic semiconductors, usually ternary systems of the type  $\text{III}_{1-x}\text{TM}_x\text{V}$  or  $\text{II}_{1-x}\text{TM}_x\text{VI}$ , where a 3d transition metal (TM) partly substitutes up to a few percent of the group III or group II cations. It has been predicted by theory that the III-nitride semiconductors GaN and InN and the II-oxide semiconductor ZnO are suitable hosts to exhibit ferromagnetism close to or above room temperature.<sup>2,3</sup> In the case of ZnO, besides V, Cr, Mn, Co, and Ni, Fe should also act as a ferromagnetic dopant.<sup>3-5</sup> Several reports on ferromagnetic systems based on ZnO can be found in the literature.<sup>1,6-14</sup> Cases in which no ferromagnetic behavior was observed,<sup>7,15-18</sup> revealed not only systematic trends for the various transition metals, doping concentrations, and differences between *n*- and *p*-type ZnO, but also conflicting results among different authors. It was thus argued<sup>11,14</sup> that experimental reproducibility needs to be improved. The exact nature of the ferromagnetism also remains unclear.<sup>1,8,11,13</sup> Among possible problems are the formation of metallic TM or TM-oxide clusters<sup>8,12-14,17</sup> or magnetism from the substrate on which thin films are deposited.<sup>18</sup> Two recent review papers on the subject concluded that there is a need for careful structural and microstructural analyses and a more precise control of the TM dopant in the oxide.<sup>1,11</sup>

Experimentally, TM dopants have been introduced both during ZnO powder synthesis<sup>10,14,16</sup> and growth of epitaxial thin films.<sup>6-9,11,15,18</sup> Ion implantation is also being actively explored for TM doping of ZnO.<sup>1,12,13,19</sup> With respect to implantation, the questions that should be clarified are: to what extent are TMs incorporated into the proper lattice sites (sub-

stituting for Zn atoms), what is the microstructure of substitutional TMs, and what are the optimum annealing conditions. We have partly addressed some of these issues in a previous study on Fe-implanted ZnO,<sup>20</sup> focusing mainly on its optical properties. In that case,  $^{56}\text{Fe}$  was implanted into ZnO single crystals at 100 keV and up to a fluence of  $10^{16} \text{ cm}^{-2}$ , followed by Rutherford backscattering spectroscopy (RBS) analysis of the damage and its recovery during thermal annealing. Since Fe in ZnO cannot be detected by RBS, particle-induced x-ray emission was used as the probing reaction, giving only limited results on the Fe lattice location. It was found that in the as-implanted state ~56% of Fe atoms were aligned with the ZnO *c* axis, increasing to ~73% following annealing in air at 1050 °C.

In this work, we have examined in detail the lattice location of radioactive  $^{59}\text{Fe}$  ( $t_{1/2}=44.6 \text{ d}$ ) in single-crystalline ZnO by means of the emission channeling technique.<sup>21</sup> Using a position-sensitive electron detector,<sup>22</sup> the angular distribution of  $\beta^-$  particles emitted by  $^{59}\text{Fe}$  was measured to provide information about the emitter lattice site. A commercially available ZnO [0001] single crystal,<sup>23</sup> grown by seeded chemical vapor transport and polished on the Zn face, was 60 keV implanted at room temperature, at the CERN/ISOLDE facility,<sup>24</sup> with the precursor isotope  $^{59}\text{Mn}$  ( $t_{1/2}=4.6 \text{ s}$ ), up to a dose of  $2.0 \times 10^{13} \text{ cm}^{-2}$ . During implantation, a 7° angle from the surface normal was applied to minimize the fraction of channeled  $^{59}\text{Mn}$  atoms, providing a well-defined depth profile (range 299 Å and straggling 136 Å).

It is important to point out that the  $^{59}\text{Mn}$   $\beta^-$  decay transfers 200 eV of recoil energy to its daughter  $^{59}\text{Fe}$ . This energy is sufficiently high to re-implant the Fe atoms, assuring in this way that they will not inherit the  $^{59}\text{Mn}$  lattice site. After implantation, the  $\beta^-$  emission channeling patterns from  $^{59}\text{Fe}$  were recorded around the [0001], [1102], [1101], and [2113] directions, providing unambiguous information about the emitter lattice site. These measurements were carried out at room temperature for the as-implanted state and following 10 min *in situ* vacuum annealing steps at 300, 600, 800, and 900 °C. A last measurement was done after a 30 min anneal-

<sup>a)</sup>Author to whom correspondence should be addressed; electronic mail: elisabete.rita@cern.ch

<sup>b)</sup>On leave at CERN-PH, 1211 Geneva 23, Switzerland.

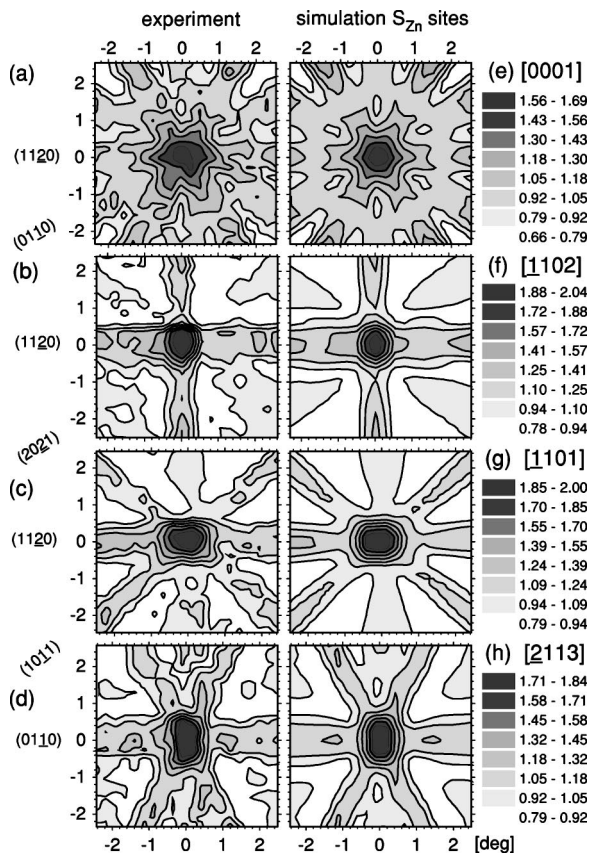


FIG. 1. Angular distribution of  $\beta^-$  particle emission yields from  $^{59}\text{Fe}$  in ZnO, around the [0001] (a), [1102] (b), [1101] (c), and [2113] (d) axes, following the 800 °C annealing. The best fits of the channeling patterns for each direction are also shown in (e)–(h) and correspond to 95(8)% of Fe atoms at  $S_{\text{Zn}}$  sites.

ing under air at 1050 °C. The subsequent evaluation of the Fe lattice location was performed by quantitatively comparing the experimental patterns with theoretical ones, using the two-dimensional fitting procedure outlined in Ref. 22. In this procedure, theoretical patterns for  $^{59}\text{Fe}$  at substitutional Zn sites ( $S_{\text{Zn}}$ ) and O sites ( $S_{\text{O}}$ ) with varying rms displacements and a diversity of interstitial sites were considered.<sup>25</sup> The  $^{59}\text{Fe}$  theoretical emission channeling patterns were calculated by means of the “many-beam” theory of electron diffraction in single crystals,<sup>21</sup> using a computational approach for  $\beta^-$  emitters in ZnO described previously.<sup>26</sup>

The experimental emission patterns along the [0001], [1102], [1101], and [2113] directions, measured following the 800 °C annealing, are shown in Figs. 1(a)–1(d). Figures 1(e)–1(h) represent the best two-fraction fits of the corresponding theoretical yields, obtained by considering Fe on substitutional  $S_{\text{Zn}}$  sites and varying its rms displacement  $u_1(\text{Fe})$ . The remaining Fe atoms are on random sites that account for sites of very low crystal symmetry or in heavily damaged surroundings, contributing with an isotropic emission yield. For this annealing temperature, the best-fit values of the  $^{59}\text{Fe}$  rms displacements from  $S_{\text{Zn}}$  sites, perpendicular to the [0001], [1102], [1101], and [2113] directions, were 0.09, 0.09, 0.08, and 0.06 Å, respectively. The corresponding fractions of Fe on  $S_{\text{Zn}}$  sites were found to be 108%, 93%, 93%, and 88%.

Figure 2 shows the substitutional Fe fractions and rms displacements as a function of annealing temperature. As can be seen, almost 90% of the Fe atoms were found on substi-

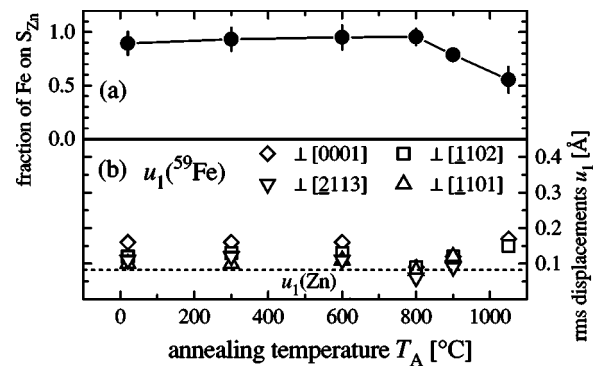


FIG. 2. Fraction of Fe atoms on substitutional Zn sites (a) and their room-temperature rms displacements perpendicular to the [0001], [1102], [1101], and [2113] crystal directions (b) following annealing steps (10 min in vacuum up to 900 °C, 30 min in air at 1050 °C). The dotted line indicates the room-temperature rms displacements of Zn atoms.

tutional Zn sites already in the as-implanted state, but with rms displacements from the ideal Zn positions of around 0.10–0.16 Å. Annealing up to 600 °C practically did not change this situation, while the 800 °C anneal induced a significant decrease of the Fe rms displacements. On the other hand, the annealing steps at 900 and 1050 °C caused not only decreases of the  $^{59}\text{Fe}$  fraction on  $S_{\text{Zn}}$  sites to 79% and 55%, respectively, but also an increase of the Fe rms displacements. Apart from the small *random* fractions, we found no evidence for  $^{59}\text{Fe}$  located at other lattice sites different from  $S_{\text{Zn}}$ .

The most remarkable feature of our experimental results is the almost perfect substitutional incorporation of Fe at Zn sites after the 800 °C annealing. The observed rms displacement values are close to the thermal vibration amplitude of the Zn atoms [ $u_1(\text{Zn})=0.082$  Å] and represent the lowest rms displacements we have found so far for any impurity in ZnO. The somewhat higher rms values observed in the as-implanted state are ascribed to the implantation damage in the surroundings of Fe, which is then largely removed during annealing at 800 °C. The fact that the substitutional Fe fraction decreases for higher annealing temperatures, accompanied by a small increase in the Fe rms displacements, may be explained as follows. High-temperature annealing is likely to introduce crystal defects in the near-surface layers, which can interact with Fe atoms, causing them to occupy lattice locations of lower symmetry. This process is possibly further enhanced by Fe diffusion at these temperatures, which would also allow for the possible formation of Fe clusters.

In previous emission channeling experiments, we investigated the lattice location of the transition metal isotopes  $^{67}\text{Cu}$  (Ref. 26) and  $^{111}\text{Ag}$  (Ref. 27) implanted in ZnO and found quite different results in terms of thermal stability of the dopant lattice site. Although the majority (60%) of  $^{67}\text{Cu}$  atoms were substitutional at  $S_{\text{Zn}}$  sites already in the as-implanted state with low rms displacements (0.16–0.17 Å), annealing above 400 °C caused a dramatic increase in the  $^{67}\text{Cu}$  rms displacements (0.3–0.5 Å) from  $S_{\text{Zn}}$  sites, along with the partial outdiffusion of Cu during the 800 °C annealing. The case of Ag was very similar to Cu, however, with maximum substitutional fractions around only 40%. In contrast, the comparably high stability of Fe against annealing is underlining the potential of ion implantation as a means of Fe doping in ZnO.

We should point out that the  $^{59}\text{Fe}$  peak concentration in our experiment was  $5.6 \times 10^{18} \text{ cm}^{-3}$  or 67 ppm, which is considerably lower than usually applied for diluted magnetic semiconductors. For instance, implants for producing ZnO diluted magnetic semiconductors were done with 250 keV  $^{55}\text{Mn}$  or  $^{59}\text{Co}$  up to fluences of  $3\text{--}5 \times 10^{16} \text{ cm}^{-2}$ , leading to concentration maxima around 3%–5%.<sup>12,13</sup> In future studies, we will therefore also explore the  $^{59}\text{Fe}$  lattice location in samples co-implanted with high doses of stable  $^{56}\text{Fe}$ .

In conclusion, we have demonstrated that for low dose implantation, the majority of the Fe atoms [95(8)%] can be incorporated on ideal substitutional Zn sites with low rms displacements (0.06–0.09 Å). There was no evidence for Fe in other regular lattice locations. While the substitutional incorporation occurs already in the as-implanted state, annealing in vacuum at 800 °C is required to promote substitutional Fe with rms displacements similar to the thermal vibration amplitude of Zn atoms. Annealing at higher temperatures, up to 1050 °C, resulted in a decrease of the substitutional Fe fraction and a small increase of the corresponding rms displacements. However, in comparison to Cu and Ag, the Fe lattice site in ZnO proved to be relatively stable at high temperatures.

This work was funded by the FCT, Portugal (project POCTI-FNU-49503-2002) and by the European Union (Large Scale Facility contract HPRI-CT-1999-00018). Two of the authors (E.R. and U.W.), acknowledge support by the FCT, Portugal.

- <sup>1</sup>S. J. Pearton, C. R. Abernathy, M. E. Overberg, G. T. Thaler, D. P. Norton, N. Theodoropoulou, A. F. Hebard, Y. D. Park, F. Ren, J. Kim, and L. A. Boatner, *J. Appl. Phys.* **93**, 1 (2003).
- <sup>2</sup>T. Dietl, H. Ohno, F. Matsukura, J. Cibert, and D. Ferrand, *Science* **287**, 1019 (2000).
- <sup>3</sup>K. Sato and H. Katayama-Yoshida, *Semicond. Sci. Technol.* **17**, 367 (2002).
- <sup>4</sup>K. Sato and H. Katayama-Yoshida, *Jpn. J. Appl. Phys., Part 2* **39**, L555 (2000).
- <sup>5</sup>M. S. Park and B. I. Min, *Phys. Rev. B* **68**, 224436 (2003).
- <sup>6</sup>K. Ando, H. Saito, Z. Jin, T. Fukumura, M. Kawasaki, Y. Matsumoto, and

- H. Koinuma, *J. Appl. Phys.* **89**, 7284 (2001).
- <sup>7</sup>Z. Jin, T. Fukumura, M. Kawasaki, K. Ando, H. Saito, T. Sekiguchi, Y. Z. Yoo, M. Murakami, Y. Matsumoto, T. Hasegawa, and H. Koinuma, *Appl. Phys. Lett.* **78**, 3824 (2001).
- <sup>8</sup>K. Ueda, H. Tabata, and T. Kawai, *Appl. Phys. Lett.* **79**, 988 (2001).
- <sup>9</sup>H. Tabata, M. Saeki, S. L. Guo, J. H. Choi, and T. Kawai, *Physica B* **308**, 993 (2001).
- <sup>10</sup>S. J. Han, J. W. Song, C. H. Yang, S. H. Park, J. H. Park, Y. H. Yeong, and K. W. Rhie, *Appl. Phys. Lett.* **81**, 4212 (2002).
- <sup>11</sup>W. Prellier, A. Fouchet, and B. Mercey, *J. Phys.: Condens. Matter* **15**, R1583 (2003).
- <sup>12</sup>D. P. Norton, S. J. Pearton, A. F. Hebard, N. Theodoropoulou, L. A. Boatner, and R. G. Wilson, *Appl. Phys. Lett.* **82**, 239 (2003).
- <sup>13</sup>N. Theodoropoulou, A. F. Hebard, D. P. Norton, J. D. Budai, L. A. Boatner, J. S. Lee, Z. G. Khim, Y. D. Park, M. E. Overberg, S. J. Pearton, and R. G. Wilson, *Solid-State Electron.* **47**, 2231 (2003).
- <sup>14</sup>Y. H. Jeong, S. J. Han, J. H. Park, and Y. H. Lee, *J. Magn. Magn. Mater.* **272**, 1976 (2004).
- <sup>15</sup>T. Fukumura, Z. Jin, M. Kawasaki, T. Shono, T. Hasegawa, S. Koshihara, and H. Koinuma, *Appl. Phys. Lett.* **78**, 958 (2001).
- <sup>16</sup>S. W. Yoon, S. B. Cho, S. C. We, S. Yoon, B. J. Suh, H. K. Song, and Y. J. Shin, *J. Appl. Phys.* **93**, 7879 (2003).
- <sup>17</sup>S. Kolesnik, B. Dabrowski, and J. Mais, *J. Appl. Phys.* **95**, 2582 (2004).
- <sup>18</sup>E. Guzmán, H. Hochmuth, M. Lorenz, H. von Wenckstern, A. Rahm, E. M. Kaidashev, M. Ziese, A. Setzer, P. Esquinazi, A. Pöppel, D. Spemann, R. Pickenhaim, H. Schmidt, and M. Grundmann, *Ann. Phys. (Leipzig)* **13**, 57 (2004).
- <sup>19</sup>S. J. Pearton, C. R. Abernathy, G. T. Thaler, R. Frazier, F. Ren, A. F. Hebard, Y. D. Park, D. P. Norton, W. Tang, M. Stavola, J. M. Zavada, and R. G. Wilson, *Physica B* **340**, 9 (2003).
- <sup>20</sup>T. Monteiro, C. Boemare, M. J. Soares, E. Rita, and E. Alves, *J. Appl. Phys.* **93**, 8995 (2003).
- <sup>21</sup>H. Hofsäss and G. Lindner, *Phys. Rep.* **210**, 121 (1991).
- <sup>22</sup>U. Wahl, J. G. Correia, A. Czermak, S. G. Jahn, P. Jaloča, J. G. Marques, A. Rudge, F. Schopper, A. Vantomme, P. Weilhammer, and The ISOLDE collaboration, *Nucl. Instrum. Methods Phys. Res. A* **524**, 245 (2004).
- <sup>23</sup>Eagle-Picher Technologies, Miami, OK 74354.
- <sup>24</sup>E. Kugler, D. Fiander, B. Jonson, H. Haas, A. Przewłoka, H. L. Ravn, D. J. Simon, K. Zimmer, and the ISOLDE collaboration, *Nucl. Instrum. Methods Phys. Res. B* **70**, 41 (1992).
- <sup>25</sup>U. Wahl, A. Vantomme, G. Langouche, J. P. Araújo, J. G. Correia, L. Peralta, and the ISOLDE collaboration, *J. Appl. Phys.* **88**, 1319 (2000).
- <sup>26</sup>U. Wahl, E. Rita, J. G. Correia, E. Alves, J. C. Soares, and the ISOLDE collaboration, *Phys. Rev. B* **69**, 012102 (2004).
- <sup>27</sup>E. Rita, U. Wahl, A. M. L. Lopes, J. P. Araújo, J. G. Correia, E. Alves, J. C. Soares, and the ISOLDE collaboration, *Physica B* **340**, 240 (2003).